Hindawi
Advances in Meteorology
Volume 2023, Article ID 5847787, 11 pages
https://doi.org/10.1155/2023/5847787

Research Article

Comparison of the Visibility Grading Forecast Method Based on Meteorological Factors and Environmental Factors

Yanyan Long, Fei Li, and Wenjun Sang

Civil Aviation Flight University of China, Guanghan 618307, China

Correspondence should be addressed to Yanyan Long; longyanyan1985@126.com

Received 2 June 2023; Revised 18 October 2023; Accepted 2 November 2023; Published 21 November 2023

Academic Editor: Stefano Federico

Copyright © 2023 Yanyan Long et al. This is an open access article distributed under the Creative Commons Attribution License, which permits unrestricted use, distribution, and reproduction in any medium, provided the original work is properly cited.

The main visibility forecast factors were identified with the support of data from routine meteorological observations from the Mianyang Airport and the Mianyang Environmental Monitoring Station from 2015 to 2018, and a visibility grading forecast model was established and tested by dint of the multiple linear regression and the KNN algorithm based on big data mining technology, and the variation characteristics of visibility in winter at the Mianyang Airport were studied. The results showed that (1) in addition to having a significant positive correlation with wind speed, the visibility in winter at the Mianyang Airport has a significant negative correlation with relative humidity, dew point temperature, AQI, $PM_{2.5}$ concentration, PM_{10} concentration, and CO, and it has the strongest correlation with relative humidity, and the correlation coefficient is −0.76. (2) The multivariate linear regression model and the KNN model were adopted for grading forecasting experiments on visibility, and the results revealed that both models could be used for visibility grading forecasts. The multiple regression model secures an accuracy of over 70% for forecasts of level 1–5 visibility. In terms of the KNN model, the forecast accuracy is the best when $K = 3$ or $K = 5$, notably for level-2, level-4, and level-5 visibility. The forecast accuracy rate is 100% for level-2 visibility, but the forecast for level-1 visibility is poor. (3) The minimum value of the average daily visibility of the Mianyang Airport in winter appeared at 09 : 00 and the maximum value appeared at 17 : 00. The level-1 visibility occurred and developed before 09 : 00 and faded and vanished between 08 : 00 and 15 : 00.

1. Introduction

Atmospheric visibility is closely related to life because low visibility can cause flight delays and induce traffic accidents, which directly affect the safety of railway, road, sailing, and air traffic [1–3]. The visibility forecast is a key part of the meteorological forecast of civil aviation airports and must be included in each forecast message. Low visibility makes it difficult for pilots to find the runway to land [4], which is a crucial factor affecting the safety and efficiency of flight and flight training, so it is of great significance to improve the accuracy of airport visibility forecasts. Visibility in civil aviation is defined as the degree of turbidity of the atmosphere or the transparency of the atmosphere. In the daytime, visibility refers to the maximum distance from which a person with normal vision (visual contrast threshold of 0.05) can see or identify a moderately sized black target from the sky background under the weather conditions at that time. In the nighttime, visibility refers to the maximum distance from which a person with normal vision (visual contrast threshold of 0.05) can see or identify a moderately sized black target from the sky background or a luminous object of moderate intensity, under the assumption that the overall illumination increases to normal daytime levels [5].

As industry and transportation develop rapidly, the emission of atmospheric pollutants has intensified, and a large number of dust, smoke, or salt particles suspended in the atmosphere seriously impact the visibility, making the study of the changing trend of visibility a popular topic worldwide [6–12]. Visibility is affected not only by local pollution but also by meteorological factors and particles [13–22]. Wen and Yeh [23] pointed out that the concentration of atmospheric pollutants has a substantial influence on visibility, and wind speed is an important meteorological parameter affecting atmospheric turbidity for it facilitates the diffusion of air pollutants. Li et al. [24] explored the association between visibility and relative humidity, wind speed, temperature, and air pressure to analyze the correlation between atmospheric visibility and meteorological elements in Dalian. Li et al. [25] discovered that atmospheric visibility varies with relative humidity and particulate concentration on a monthly and daily basis. Li et al. [26] noted that the decline in visibility in the Sichuan Basin is mainly caused by PM. While analyzing the causes of impact on visibility, some scholars have also built visibility forecasting models. Li et al. [27] employed the statistical-dynamic method and developed a visibility forecasting equation on the basis of the meteorological concept model. Liang and Hou [28] used the forecast factor index method to forecast visibility, and concluded that visibility had a strong correlation with humidity, temperature, and wind speed. Some scholars used diagnostic analysis methods to develop visibility forecasting equations. Hu et al. [29] adopted neural network step-by-step classification modeling to forecast visibility. Shu et al. [30] employed the least squares method to create a dynamic-statistical model of visibility forecasting in Shanghai with the support of historical data on visibility and atmospheric pollutants. Zhou et al. [31] used MM5 numerical forecasting products to establish regression equations and provide low-visibility grading forecasts. The weather research and forecasting (WRF) model was utilized by Li et al. [32] to statistically simulate fog production.

Although scholars both at home and abroad have conducted a lot of research on visibility forecasting with different methods, the accuracy of current visibility forecast can still not reach 100% due to the complexity of the weather, and it is necessary to continuously explore fresh ideas and methods for visibility forecast research in order to improve the accuracy of forecasting. In view of the complexity of visibility forecasting and various impact factors of visibility in different regions, the visibility grading forecast of the flight training airport in the Civil Aviation Flight University of China will be studied in this paper. The flight training airport at the Civil Aviation Flight University of China is located in the Mianyang city, Sichuan Province, which is the same airport as the Mianyang Airport (hereinafter referred to as Mianyang Airport), and mainly undertakes flight teaching tasks for primary teaching aircraft, medium-sized teaching aircraft, and high-level teaching aircraft. Since the airport is in the Sichuan Basin, the relative humidity is high, and low visibility events are common in the winter, which affects the safety and efficiency of flight training [33], so it is necessary to study the factors affecting visibility in winter, build a forecast model, and provide a reference for flight training support. In this paper, with the support of data from routine meteorological observations from the Mianyang Airport and the Mianyang Environmental Monitoring Station, the visibility grading forecast model in winter is constructed by dint of multiple linear regression and the KNN algorithm based on big data mining technology, according to the flight training needs. The two forecast models are tested and comparatively analyzed, in order to provide a reference for the visibility grading forecast at the training airport and an objective product for visibility forecast and early warning.

2. Materials and Methods

2.1. Sources of Materials. The meteorological observation data used in this paper are collected from the hourly monitoring data provided by the Automated Weather Observing Systems (AWOS) from 2015 to 2018, including air pressure, corrected sea level pressure, temperature, relative humidity, dew point temperature, total cloud cover, low cloud cover, wind (wind direction and wind speed), and visibility. The height of the air pressure data is the runway elevation. The height of the corrected sea level pressure data is the sea level height. The height of the temperature data is 1.5 meters above the ground. The height of the relative humidity data is 1.5 meters above the ground. The height of dew point temperature data is 1.5 meters above the ground. The height of wind speed data is 10 meters above the ground. Environmental data were collected from the Mianyang Environmental Monitoring Station from 2015 to 2018, including data from four monitoring sites: Fule Mountain (104.778°E, 31.4747°N), High-tech Zone Water Utility (104.6717°E, 31.4656°N), Mianyang No. 3 Waterworks (104.7283°E, 31.5072°N), and Mianyang Municipal People's Congress (104.7536°E, 31.4539°N), and hourly data of environmental factors, including AQI (air quality index), $PM_{2.5}$, PM_{10}, NO_2, SO_2, CO, and O_3.

In this paper, the quality of the aforementioned data is well controlled, the data format is unified, the missing measurement and abnormal data are eliminated, and the interpolation method is also used to interpolate the data. Due to the inconsistencies in data dimensions, the data are standardized in this paper.

2.2. Research Methods

2.2.1. Multiple Linear Regression Model. The linear regression model with the dependent variable y and the independent variables $x_1, x_2, \ldots, x_p$ is

$$y = \beta_0 + \beta_1 x_1 + \beta_2 x_2 + \cdots + \beta_p x_p + \varepsilon, \tag{1}$$

where $\beta_0, \beta_1, \ldots, \beta_p$ denote unknown parameters, β_0 is the regression constant, $\beta_1, \ldots, \beta_p$ refer to the regression coefficient, and ε signifies a random error. When $p \geq 2$, the model is called a multivariate linear regression model.

2.2.2. KNN Algorithm. In recent years, the KNN algorithm has attracted much attention in the field of meteorology. As one of the ten classic algorithms of data mining, it is a nonparametric supervision algorithm proposed by Cover and Hart [34], and a nonparameter estimation technology for classification through the calculation of the distance between different eigenvalues of objects. This rapidly developing practical data mining technology has applications in precipitation forecasting [35], wind forecasting [36–38], and cloud classification [39]. The idea is that if the majority of K most similar (the closest proximity) samples in the feature space belong to a certain category, then the sample also belongs to that category, where K is usually an integer not greater than 20. In the KNN algorithm, the selected neighbors are objects that have been correctly categorized. The principle of KNN is to calculate the distance between the sample to be labeled and each sample in the dataset, and take the nearest K samples. The category of samples to be labeled is determined through a vote based on K nearest samples.

The K nearest neighbor algorithm system design is as follows: 1. calculate the distance. In this paper, the Euclidean distance method is used to measure the distance. 2. Choose a neighbor. For each sample to be classified, the distance between it and the training sample is calculated, and the nearest K samples are selected as their neighbors. K is determined by cross-validation. 3. Determine the category. According to the categories of K neighbors, the categories of samples to be classified are determined by majority voting.

The concrete steps are as follows: suppose there is a set of historical weather sample sets defined as S. S consists of i weather samples, and each weather sample consists of m attribute variations and 1 label quantity. Its mathematical expression is

$$S = \left\{ \begin{array}{c} [X_{11}, X_{12}, X_{13}, \cdots, X_{1m}, L_1] \\ [X_{21}, X_{22}, X_{23}, \cdots, X_{2m}, L_2] \\ [\cdots\cdots\cdots\cdots\cdots\cdots\cdots\cdots\cdots] \\ [X_{i1}, X_{i2}, X_{i3}, \cdots, X_{im}, L_i] \end{array} \right\}. \tag{2}$$

In this paper, the attribute variable X_{ij} represents six factors, namely, AQI, $PM_{2.5}$, PM_{10}, relative humidity, dew point temperature, and wind speed. L_i is called the label quantity, and the label quantity refers to the visibility level. The mathematical model for predicting visibility level by dint of the KNN algorithm is as follows: we suppose that the set of six elements of AQI, $PM_{2.5}$, PM_{10}, relative humidity, dew point temperature, and wind speed on the forecast day is $Y_i = (y_1, y_2, \ldots, y_m)$, which is called the prediction sample. When conducting the forecast, we first find K nearest neighbors that are most similar to the prediction sample Y_i in the training sample set S (K is usually an odd number); Then, we find the set of K label quantities (visibility levels) $L = (L_1, L_2, \ldots, L_k)$. Finally, in accordance with the majority rule in voting, L_i was selected as the prediction result of the prediction sample Y_i.

2.3. Visibility Grading Standard. Visibility is a major factor influencing general aviation flight training, and its value can determine whether captain training or solo training is conducted. Winter has the highest number of low-visibility days and has the greatest impact on flight training. In order to better provide flight training support and accurate visibility forecast, the visibility is graded according to the aircraft flight standards. Visibility grading forecast has emerged as a new topic in recent years [31, 40, 41], but there are no grading standards in place. In this paper, visibility is divided into five levels according to the aircraft flight standards (Table 1), with 800 m, 1,600 m, 2,000 m, and 5,000 m as the demarcation values based on the level of visibility.

3. Visibility Grading Forecasting Methods of the Mianyang Airport in Winter and Its Characteristics

3.1. Correlation Analysis of Visibility with Each Parameter in Winter. Since low visibility events occur most frequently in winter (December, January, and February) and affect the safety and efficiency of flight training, this paper focuses on the winter visibility at the Mianyang Airport. 14 meteorological factors and environmental factors were selected for analysis on their correlation with corresponding visibility, and the correlation coefficients were obtained. Those factors with correlation coefficients greater than or equal to 0.3 were taken as high-impact physical quantities and passed the significance level test of $a = 0.05$.

Figure 1 shows the correlation coefficients between winter visibility and meteorological factors at the Mianyang Airport, and the analysis results reveal that the correlation coefficients between visibility and relative humidity, dew point temperature, and wind speed are high. Among all factors, relative humidity has a strong negative correlation with visibility, and the correlation coefficient is −0.76. Visibility and dew point temperature are strongly adversely connected (the correlation coefficient: −0.55), while visibility and wind speed are significantly positively correlated (the correlation coefficient: 0.33).

Relative humidity has a strong negative correlation with visibility, and with the increase in relative humidity, visibility gradually decreases. This is because with the increase in relative humidity, the radius of wet particles increases, the extinction increases, and the visibility decreases. Dew point temperature has a strong negative correlation with visibility, and with the increase in dew point temperature, visibility gradually decreases. This is because the dew point temperature is high and the water vapor content is high, which will lead to a decrease in visibility. Relative humidity and dew point temperature have the greatest correlation with visibility, which also shows that the change in visibility in this airport is most influenced by these two factors and it is also the focus of visibility forecast. Other factors do not change much, so the correlation is also small.

Figure 2 presents the correlation coefficients between visibility in winter at the Mianyang Airport and environmental factors in four different monitoring sites in Mianyang city. The analysis shows that the environmental factors of the Municipal People's Congress are more indicative of the visibility of Mianyang Airport, and the Municipal People's Congress is located 3.09 km to the northeast of the Mianyang Airport. To be specific, the following indexes have a strong correlation with visibility at the Municipal People's Congress: AQI has a significant negative correlation with visibility and the correlation coefficient is −0.59; $PM_{2.5}$ concentration has a significant negative

Table 1: Visibility grading standard.

Visibility level	Meteorological visibility (m)	Aircraft flight standard
1	vis ≤ 800	When visibility is less than or equal to 800 m, all aircraft cannot take off
2	800 < vis ≤ 1,600	When visibility is greater than 800 m, twin-engine turbo, three-engine turbo, and four-engine turbo aircrafts can take off
3	1,600 < vis ≤ 2,000	When visibility is greater than 1,600 m, one-engine and twin-engine aircrafts can take off
4	2,000 < vis ≤ 5,000	When visibility is greater than 2,000 m, students can participate in the flight training
5	vis > 5,000	When visibility is greater than 5,000 m, the student can fly an aircraft alone

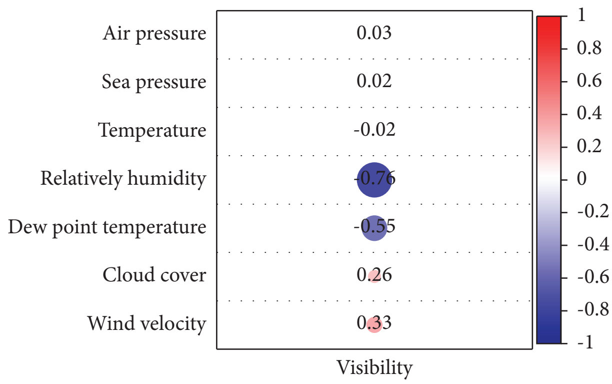

Figure 1: Correlation coefficients between visibility and meteorological factors.

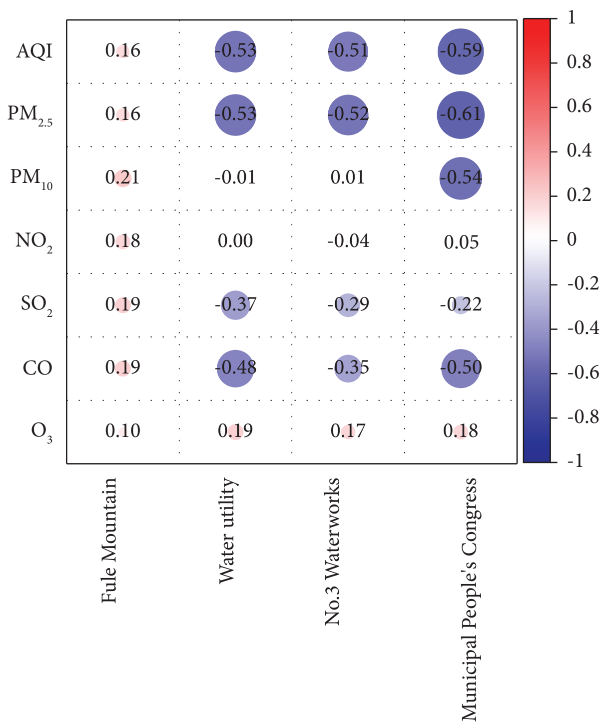

Figure 2: Correlation coefficients between visibility and environmental factors.

correlation with visibility and the correlation coefficient is −0.61; PM_{10} concentration has a significant negative correlation with visibility and the correlation coefficient is −0.54. Visibility correlates more significantly with $PM_{2.5}$ concentrations than with PM_{10} concentrations. Visibility is also significantly inversely correlated with CO, with a correlation coefficient of −0.5.

Figure 3 is a scatter plot for the relationships between visibility and various meteorological factors. Figure 3(a) shows that the relationship between visibility and relative humidity can be represented by $y = -0.0031x + 97.568$ (y is visibility and x is relative humidity). As the relative humidity increases, the visibility gradually decreases, and the relative humidity directly improves the scattering efficiency by affecting the moisture absorption growth of the particles, thus reducing the visibility. Figure 3(b) shows that with the increase in dew point temperature, which indicates the increase in water vapor content, visibility gradually decreases, and the fitting relationship can be represented by $y = -0.0006x + 5.8168$ (y is visibility and x is dew point temperature). Figure 3(c) demonstrates that as the wind speed increases, the better the diffusion conditions become, and the visibility gradually increases. Lower wind speeds do not promote the dispersion of pollutants and result in lower visibility. When the wind speed is less than or equal to 2 m/s (that is, a small wind speed in the traditional sense), the visibility is generally less than 10 km, and when the wind speed is greater than 3 m/s, the visibility is better.

Figure 3(d) shows that AQI and visibility can be fitted through the following relationship formula: $y = 157.68e^{-1E-4x}$ (y is visibility and x is AQI index), and R square is 0.3937, indicating that the fitting effect is great. It can also be found from the figure that as the AQI index increases, the visibility decreases. When the AQI is less than 100, the visibility slowly decreases as the index increases, and conversely, when the AQI is more than 100, the visibility decreases drastically as the index increases. Figure 3(e) demonstrates that the relationship between $PM_{2.5}$ and visibility can be represented through the following formula: $y = 122.59e^{-1E-4x}$ (y is visibility and x is $PM_{2.5}$ concentration), and R square is 0.4208, indicating that the fitting effect is great. It can also be found from the figure that as the $PM_{2.5}$ concentration increases, the visibility decreases. Excessive $PM_{2.5}$ concentration may lead to low visibility. When the $PM_{2.5}$ concentration is less than 70 μg/m^3, the visibility slowly decreases as the concentration increases, and conversely, when the $PM_{2.5}$ concentration is more than 70 μg/m^3, the visibility decreases drastically as the concentration increases. Figure 3(f) shows that PM_{10} and visibility can be fitted through the following relationship formula: $y = 163.09e^{-1E-4x}$ (y is visibility and x is PM_{10} concentration). It can also be found from the figure that as the

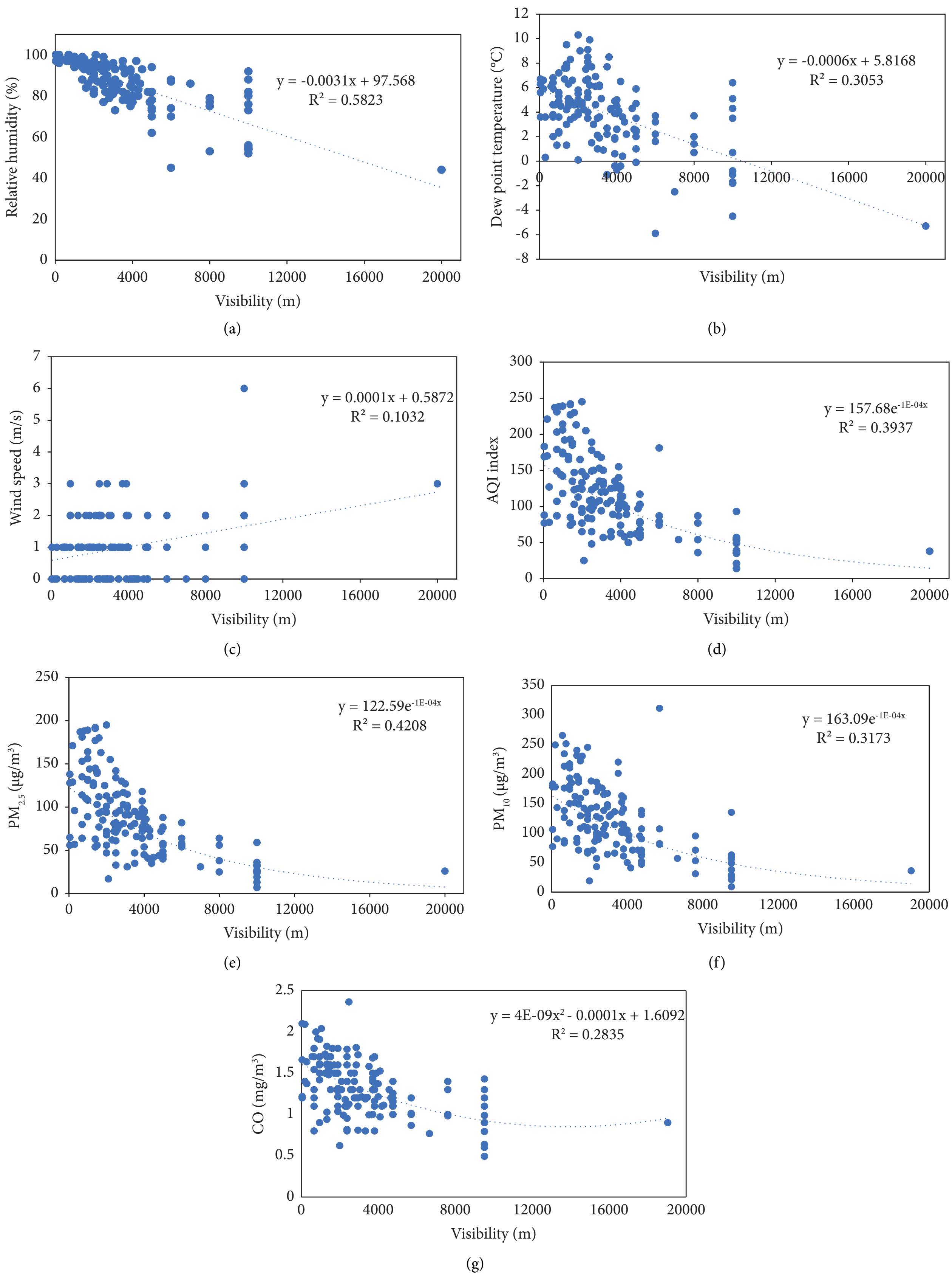

Figure 3: Scatter plot for the relationships between visibility and various meteorological factors: (a) relative humidity, (b) dew point temperature, (c) wind speed, (d) AQI, (e) $PM_{2.5}$ concentration, (f) PM_{10} concentration, and (g) CO.

PM_{10}concentration increases, the visibility decreases. When the PM_{10} concentration is less than $100\,\mu g/m^3$, the visibility slowly decreases as the concentration increases, and conversely, when the PM_{10} concentration is more than $100\,\mu g/m^3$, the visibility decreases drastically as the concentration increases. Figure 3(g) shows that the relationship between CO and visibility can be represented by $y = 4E - 9x^2 - 0.0001x + 1.6092$ (y is visibility and x is CO concentration). It can also be found from the figure that visibility below 10 km decreases as the CO concentration increases.

3.2. Multiple Linear Regression Models and Tests. Based on the results of the correlation analysis between visibility and each factor, the multivariate linear regression model is used to establish the visibility grading forecast equation, and after repeated introduction and deletion of parameters, six parameters are selected for modeling optimization for corresponding visibility level, and the visibility grading forecast model is obtained (Table 2), where Y is the forecast value of visibility, X_1 is AQI, X_2 is $PM_{2.5}$, X_3 is PM_{10}, X_4 is relative humidity, X_5 is the dew point temperature, and X_6 is the wind speed.

A comparative analysis of forecast and observation was carried out by dint of the visibility grading forecast model. As can be seen in Figure 4, the trend of the forecast and that of the observation are consistent, indicating that the visibility grading forecast model has a better simulation effect.

In order to objectively evaluate the visibility forecast results, based on visibility observations, the forecast accuracy rate P_C, the underreport rate P_O, and the false report rate F_{AR} are calculated to evaluate the forecasting capability of the model. The formulas are as follows:

$$
\begin{aligned}
P_C &= \frac{N_A}{(N_A + N_B + N_C)} \times 100\%, \\
P_O &= \frac{N_B}{(N_A + N_B)} \times 100\%, \\
F_{AR} &= \frac{N_C}{(N_A + N_C)} \times 100\%,
\end{aligned}
\tag{3}
$$

where N_A is the correct number of forecasts, N_B is the number of missing reports, and N_C is the number of false reports.

Table 3 shows that the visibility grading forecast model has an accuracy of 75% for level-1 visibility forecasting, 70% accuracy for level-2 visibility forecasting, 75% accuracy for level-3 visibility forecasting, 84.6% accuracy for level-4 visibility forecasting, and 95.8% accuracy for level-5 visibility forecasting. The rate of missing and false reports is less than 30%. Level-5 visibility forecasting is more accurate because level-5 visibility is better, with a value greater than 5,000 m. This kind of weather is generally relatively stable and it is less affected by the changes of meteorological factors and environmental factors. Level-2 visibility forecasting is the lowest, because level-2 visibility is relatively low, with the value between 800 m and 1,600 m. At this time, the weather is unstable, and it is in the stage of inversion layer destruction, which is greatly influenced by the changes in meteorological factors and environmental factors, so the forecast is more difficult and the forecast is the lowest.

Based on the multivariate linear regression visibility grading forecast model, the forecast effect is good, and it is obviously better than the nongrading model. In the experiment, the visibility nongrading forecast model has an accuracy of 16.7% for level-1 visibility forecasting, 20% accuracy for level-2 visibility forecasting, 16.7% accuracy for level-3 visibility forecasting, 55.9% accuracy for level-4 visibility forecasting, and 90.5% accuracy for level-5 visibility forecasting. So, the visibility grading forecast model has a higher accuracy and it can provide a reference for visibility grading forecasting, and this is also a basic method for the interpretation and application of current numerical weather prediction.

3.3. KNN Model and Test. Due to the chaotic and nonlinear nature of atmospheric motion, it is difficult to accurately describe and simulate weather models with one equation or a set of simple linear or nonlinear regression equations. In this paper, we also try to use the KNN algorithm to establish a grading visibility forecasting model.

In this paper, the K value is determined by cross-validation. Table 4 shows the classification accuracy when $K = 3$, 4, and 5. The results demonstrate that when $K = 3$ or $K = 5$, the cross-validation accuracy rate of visibility forecasting is 70%, and the rate is only 63.5% when $K = 4$. When $K = 3$ or $K = 5$, the accuracy rate is better, in comparison to the rate when $K = 4$. Therefore, $K = 3$ is used to build the KNN model.

To understand the predictive performance of the KNN classifier on the visibility of each level, Table 5 further shows the cross-validation results of the KNN classifier for each level of visibility classification. The horizontal axis in the table represents the forecast of visibility at all levels, the vertical axis represents the observation of visibility at all levels, and the cross line represents the forecast accuracy.

It can be seen from the table that the KNN classifier performs better in high-visibility weather. The accuracy rate is as high as 75% for the observation visibility greater than 5,000 m (level 5), and as high as 77.8% for observation visibility greater than 2,000 m but not greater than 5,000 m (level 4). In medium-visibility weather, the KNN classifier forecasts a one-level lower visibility. When the observation visibility is level 3, the forecast is level 2, so we can conclude that the visibility forecast value is lower than the observation. The KNN classifier performed very well in low-to-medium-visibility weather. When the observation visibility is greater than 800 m but not greater than 1,600 m (level 2), the accuracy rate reaches as high as 100%. The KNN classifier performs poorly in low-to-medium-visibility weather. When the observation visibility is not greater than 800 m (level 1), the accuracy rate is only 33.3%.

The possible reason for poor calculations for low-visibility weather is that there are many influencing factors in low-visibility weather. (1) In the vertical space, in addition to influencing factors such as temperature,

Table 2: Visibility grading forecast model.

Level	Visibility grading forecast model
1	$Y = 16937.11 - 3.50972X_1 + 25.05609X_2 - 16.386X_3 - 165.969X_4 + 32.58018X_5 + 95.8339X_6$
2	$Y = 5183.243 - 20.0912X_1 + 7.546235X_2 + 13.8712X_3 - 41.6568X_4 + 33.85167X_5 + 20.06746X_6$
3	$Y = 3196.879 - 30.872X_1 + 43.75235X_2 - 5.32392X_3 - 9.30138X_4 + 4.731934X_5 - 73.6623X_6$
4	$Y = 12996.76 - 16.4763X_1 - 3.28072X_2 + 3.422158X_3 - 87.6827X_4 - 76.9059X_5 - 64.8086X_6$
5	$Y = 18171.71 - 189.568X_1 + 94.9773X_2 + 47.38879X_3 - 71.2293X_4 - 345.517X_5 + 446.3217X_6$

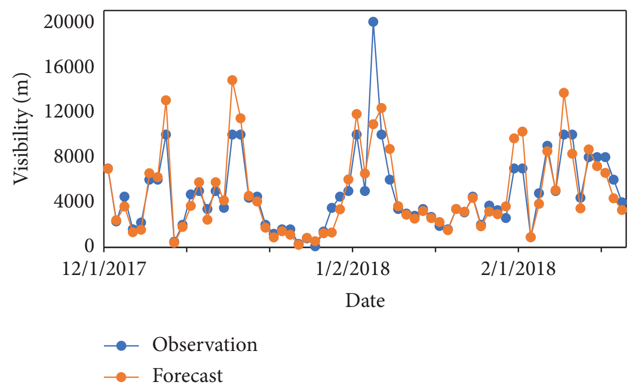

Figure 4: Forecast and observation comparison through the visibility grading forecast model.

Table 3: Visibility grading forecast model test.

Visibility level	P_C (%)	P_O (%)	F_{AR} (%)
1	75	25	0
2	70	0	30
3	75	25	0
4	84.6	8.3	8.3
5	95.8	4.2	0

Table 4: KNN algorithm accuracy through cross-validation when different values are taken (unit: %).

K value	$K = 3$ (%)	$K = 4$ (%)	$K = 5$ (%)
Accuracy	70.0	63.5	70.0

Table 5: Cross-validation results of KNN classifiers for all levels of visibility (unit: %).

Forecast observation	Level 1 (%)	Level 2 (%)	Level 3 (%)	Level 4 (%)	Level 5 (%)
Level 1	33.3	33.3	0.0	33.3	0.0
Level 2	0.0	100.0	0.0	0.0	0.0
Level 3	0.0	100.0	0.0	0.0	0.0
Level 4	14.8	7.4	0.0	77.8	0.0
Level 5	0.0	0.0	0.0	25.0	75.0

pressure, humidity, wind, and AQI, the temperature profile within the boundary layer is also a significant influencing factor. For example, fog and heavy pollution weather at airports are often accompanied by the phenomenon of "temperature inversion," which puts a lid on the vertical diffusion of pollutants. (2) In the horizontal space, in addition to local pollutants and water vapor and other influencing factors, pollutants or water vapor transportation in the surrounding area may also have an impact on local visibility. (3) From the perspective of the time series, the continuous accumulation of pollutants or water vapor also has a greater influence on the low-visibility weather. For instance, on day 1, day 2, and day 3, all meteorological factors (high humidity and small wind) are the same, but the visibility gradually decreases as time goes by. What was not taken into account in the analysis include temperature inversions in the vertical space, contaminant transport in the horizontal direction, and cumulative effects in terms of time series, which may become possible causes of unsatisfactory forecasts for the low-visibility weather.

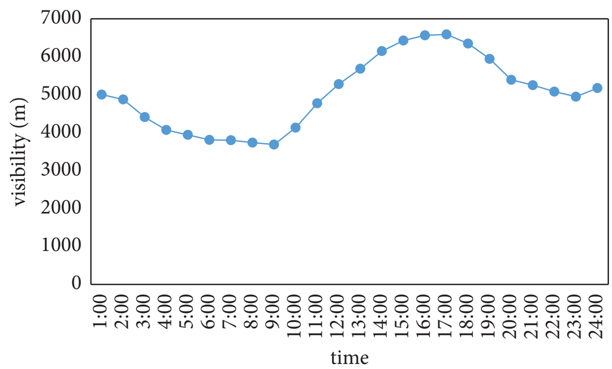

Figure 5: Daily variation of average visibility in winter.

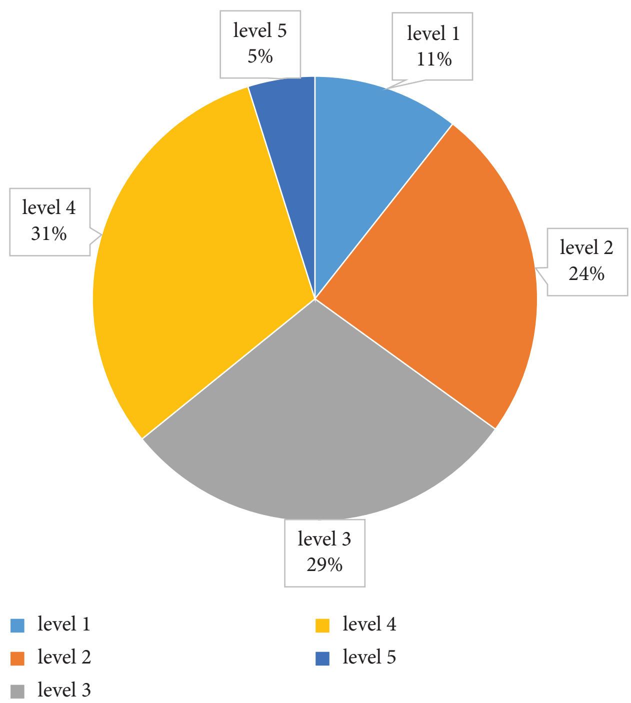

Figure 6: Proportion of visibility at all levels in winter.

3.4. Analysis of Visibility Characteristics of the Mianyang Airport in Winter. Based on the visibility data, the variation of average daily visibility in winter at the Mianyang Airport is analyzed (Figure 5). The daily variation of average visibility at the Mianyang Airport is obvious, with the minimum value of daily visibility appearing at 9 : 00 (Beijing time, the same as below) and the maximum value appearing at 17 : 00. The average low value of visibility appeared at 4 : 00 to 9 : 00 in the morning. The visibility began increasing slowly from 9 : 00, reached the maximum value at 17 : 00, and then decreased slowly.

The weather that affects visibility in Mianyang Airport in winter is mainly radiation fog. Radiation fog has obvious daily variation, which mainly occurs in the morning and generally lasts until noon and afternoon. The formation of radiation fog is mainly due to the ground radiation cooling at night, so it is easier to produce radiation fog in the morning, resulting in low visibility. As the sun rises, the intensity of solar radiation increases, the ground temperature increases, the cooling effect of ground radiation begins to weaken, the dew point deficit increases, the water vapor content near the ground decreases, the intensity of radiation fog decreases, and the visibility is greatly improved. At the same time, the height of the inversion layer rises further, which is beneficial to the diffusion of water vapor in the lower layer, and also reduces the relative humidity and increases the visibility. Therefore, the visibility at noon is generally greater than that in the morning, until it reaches its maximum at 17 : 00.

The visibility at all levels in winter was analyzed (Figure 6). Days of level-5 visibility were the least, which accounted for 5% of the total. The proportion of days with level-4 visibility was 31%, which is the highest, followed by days with level-3 visibility at 29%, days with level-2 visibility at 24%, and days with level-1 visibility at 11%. This indicates that low visibility does not occur very often, but it is the most critical level affecting flight training.

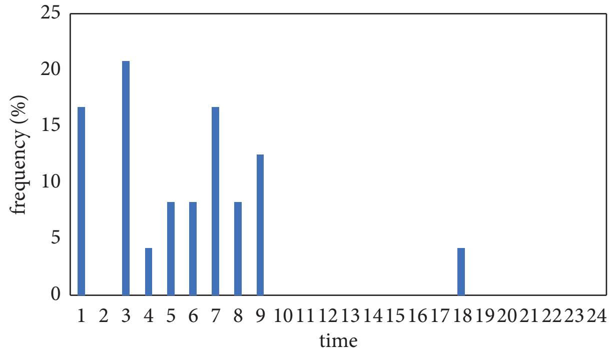

(a)

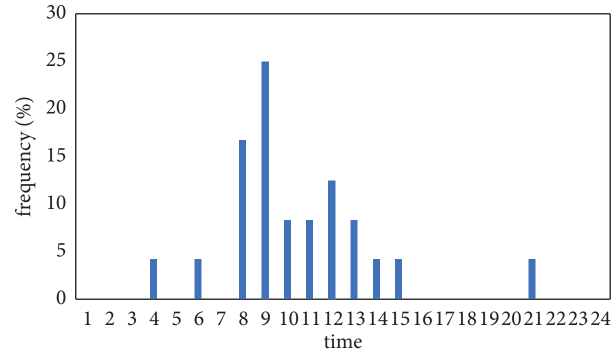

(b)

Figure 7: Occurrence time-frequency (a) and disappearing time-frequency (b) of visibility below 800 m.

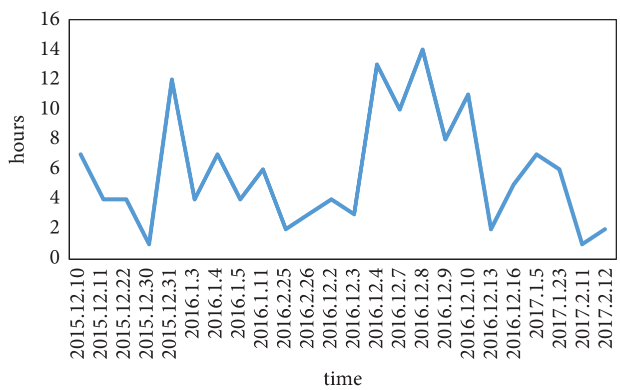

Figure 8: Visibility duration below 800 m.

Since level 1 is the most important level for flight training, so we analyzed the occurring and disappearing of the visibility below 800 m, and the period of visibility that is most likely to develop or fade in a day, which lays a groundwork for the visibility forecast below 800 m.

As can be seen from Figure 7, visibility below 800 m mainly occurred and developed before 09 : 00, and the occurrence frequency is the highest at 03 : 00, indicating that low visibility tends to occur in the early morning. There are three peak periods (01 : 00, 03 : 00, and 07 : 00) for visibility occurrence below 800 m. As for the visibility disappearing time below 800 m, 08 : 00 to 15 : 00 is the peak period for visibility to diminish and dissipate, with 09 : 00 being the time for most dissipation, and most of low visibility dissipates before 15 : 00.

Visibility below 800 m occurs 24 times in total, and its duration is analyzed (Figure 8). The longest duration was 14 hours, which occurred on December 8, 2016, followed by 13 hours on December 4, 2016. In December 2016, low visibility lasted longer and occurred in more days in December 2016 than in other months.

4. Conclusions

In this paper, the relationship between winter visibility and meteorological factors and environmental factors is studied. The authors construct a visibility grading forecast model in winter by dint of the multiple linear regression and the KNN algorithm based on big data mining technology, and perform the testing and comparative analysis. At the same time, the visibility characteristics in winter at the Mianyang Airport are analyzed. The conclusions are drawn as follows:

(1) Mianyang Airport's winter visibility has a significant correlation with relative humidity, dew point temperature, wind speed, AQI, $PM_{2.5}$ concentration, PM_{10} concentration, and CO. It has a significant positive correlation with wind speed, and a significant negative correlation with relative humidity, dew point temperature, AQI, $PM_{2.5}$ concentration, PM_{10} concentration, and CO, of which relative humidity has the largest impact on the visibility with a correlation coefficient of −0.76. The correlation coefficient of dew point temperature is −0.55, the correlation coefficient of wind speed is 0.33, the correlation coefficient of AQI at the Municipal People's Congress is −0.59, the correlation coefficient of $PM_{2.5}$ concentration is −0.61, the correlation coefficient of PM_{10} concentration is −0.54, and the correlation coefficient of CO is −0.5.

(2) The multivariate linear regression model and the KNN model were adopted to conduct grading forecasting experiments on visibility, respectively, and the results showed that both models can be used for visibility grading forecasts, but the forecast effect for different levels of visibility is different. The multiple regression model can provide great level-1, level-2, level-3, level-4, and level-5 visibility forecasts, with an accuracy rate of more than 70%. The KNN model has a better grading accuracy rate at $K = 3$ or $K = 5$ than at $K = 4$, and the KNN model can better forecast level-2, level-4, and level-5 visibility. Note that, the accuracy rate of level-2 visibility is 100%. However, the forecast performance is poor in the case of low visibility (level 1). In practice, the two models can complement each other to further increase the accuracy of the forecast.

(3) At the Mianyang Airport, the minimum value of average daily visibility in winter appeared at 09 : 00,

the maximum value appeared at 17 : 00, and the average low value of visibility appeared from 04 : 00 to 09 : 00 in the morning. According to the statistical analysis of visibility at all levels in winter, level-5 visibility days account for the least proportion of the total, and most are level-4 visibility days. Level-1 visibility occurred and developed before 09 : 00, 01 : 00, 03 : 00, and 07 : 00 and these were the peak time for the occurrence of level-1 visibility, and 08 : 00–15 : 00 was the peak period for the visibility to diminish and dissipate. The maximum duration of level-1 visibility was 14 hours.

In the future, we will also work in the following areas: first, collecting vertical space data and including the temperature inversion into forecast factors; second, taking into account the transport, convergence, and dispersion of surrounding pollutants and water vapor; third, considering the cumulative effect of pollutants and water vapor, in hope of improving the effects of the KNN classifier and increasing the forecast accuracy.

Data Availability

The [meteorological and environmental] data used to support the findings of this study are available from the first author upon request.

Conflicts of Interest

The authors declare that they have no conflicts of interest.

Authors' Contributions

Long Yanyan contributed mainly to this work. Li Fei and Sang Wenjun provided support.

Acknowledgments

This research was supported by the National Natural Science Foundation of China (42105087), the Science Research Fund Key Project of the Civil Aviation Flight University of China (ZJ2016-02), the Science Research Fund project of the Civil Aviation Flight University of China (J2019-051), and the Civil Aviation Flight Technology and Flight Safety Research Base Project (F2018KF04).

References

[1] Dgca, "Handbook on civil aviation statistic—glimse of aviation statistic 2017–2018," 2018, https://www.scribd.com/document/430990162/HANDBOOK-2017-18-docx.

[2] A. K. Sharma, "Philosophy-and-political-advocacy," annual_report_15, National Council of Applied Economic Research, Indraprastha Estate, New Delhi, India, 2012,http://www.ncaer.org/uploads/annualreport/pdf/annual_report_15_Annual_Report_NCAER2013.pdf.

[3] DGCA, "Report of Working Group on Civil Aviation for Formulation of Twelfth Five Year Plan (2012–2017)," Committees Reports, DGCA, New Delhi, India, 2019,http://dgca.nic.in/aic/aic08_07.pdf.

[4] J. M. Hanesiak and X. L. Wang, "Adverse-weather trends in the Canadian arctic," *Journal of Climate*, vol. 18, no. 16, pp. 3140–3156, 2005.

[5] Civil Aviation Administration of China, *Norm for meteorological ground observation of civil aviation*, Civil Aviation Administration of China, Beijing, China, 2021.

[6] M. Doyle and S. Dorling, "Visibility trends in the UK 1950–1997," *Atmospheric Environment*, vol. 36, no. 19, pp. 3161–3172, 2002.

[7] N. M. Mahowald, J. A. Ballantine, J. Feddema, and N. Ramankutty, "Global trends in visibility: implications for dust sources," *Atmospheric Chemistry and Physics*, vol. 7, no. 12, pp. 3309–3339, 2007.

[8] Y. I. Tsai, S.-C. Kuo, W.-J. Lee, C.-L. Chen, and P.-T. Chen, "Long-term visibility trends in one highly urbanized, one highly industrialized, and two rural areas of Taiwan," *Science of the Total Environment*, vol. 382, no. 2-3, pp. 324–341, 2007.

[9] H. Che, X. Zhang, Y. Li, Z. Zhou, and J. J. Qu, "Horizontal visibility trends in China 1981–2005," *Geophysical Research Letters*, vol. 34, no. 24, 2007.

[10] D. Chang, Y. Song, and B. Liu, "Visibility trends in six megacities in China 1973–2007," *Atmospheric Research*, vol. 94, no. 2, pp. 161–167, 2009.

[11] F. S. Syed, H. Kornich, and M. Tjernstrom, "On the fog variability over south Asia," *Climate Dynamics*, vol. 39, no. 12, pp. 2993–3005, 2012.

[12] J. Zhang, P. G. Zhao, X. T. Wang et al., "Main factors influencing winter visibility at the xinjin flight college of the civil aviation flight university of China," *Advances in Meteorology*, vol. 2020, Article ID 8899750, 13 pages, 2020.

[13] J. C. Chow, J. D. Bachmann, S. S. G. Wierman et al., "Visibility: science and regulation," *Journal of the Air & Waste Management Association*, vol. 52, no. 9, pp. 973–999, 2002.

[14] K. Du, C. Mu, J. Deng, and F. Yuan, "Study on atmospheric visibility variations and the impacts of meteorological parameters using high temporal resolution data: an application of Environmental Internet of Things in China," *The International Journal of Sustainable Development and World Ecology*, vol. 20, no. 3, pp. 238–247, 2013.

[15] J. Wang and X. Liu, "The discuss on relationship between visibility and mass concentration of PM2.5 in Beijing," *Acta Meteorologica Sinica*, vol. 6, no. 2, pp. 221–228, 2006.

[16] S. Y. Gong and J. L. Feng, "Relationships among relative humidity, PM10 concentration and atmospheric visibility in Shanghai," *Research of Environmental Sciences*, vol. 25, no. 6, pp. 628–632, 2012.

[17] H. Bian, S. Q. Han, Y. F. Zhang, Y. C. Feng, J. H. Wu, and Q. Yao, "Relationship between atmospheric visibility and particulate matter pollution in Tianjin," *China Environmental Science*, vol. 32, no. 3, pp. 406–410, 2012.

[18] H. M. Pan, D. Wu, and F. Li, "The relationship between atmospheric visibility and particulate matter in Guangzhou," *Environmental Monitoring and Forewarning*, vol. 7, no. 1, pp. 32–36, 2015.

[19] Y. Yan, Y. C. Miao, J. Li, and J. P. Guo, "Meteorological characteristics of prolong low-visibility events in Haikou during February 2018," *Acta Scientiarum Nauralium Universitaties Pekinensis*, vol. 55, no. 5, pp. 899–906, 2019.

[20] H. P. Liu, P. L. Dai, Q. Z. Zhang, X. F. Guo, and C. M. Hou, "Features of atmospheric visibility and its influence with the air pollution in Zhengzhou," *Meteorological and Environmental Sciences*, vol. 31, no. 4, pp. 44–46, 2008.

[21] W. L. Zhang, F. C. You, X. L. Zhang, and S. Y. Fan, "Meteorological characteristics analysis of severe haze weather

processes in Beijing in January 2013," *Meteorological and Environmental Sciences*, vol. 39, no. 2, pp. 46–54, 2016.

[22] Y. Z. Chen, D. Zhao, F. H. Chai et al., "Correlation between the atmospheric visibility and aerosol fine particle concentrations in Guangzhou and Beijing," *Chinese Environmental Science*, vol. 30, no. 7, pp. 967–971, 2010.

[23] C.-C. Wen and H.-H. Yeh, "Comparative influences of airborne pollutants and meteorological parameters on atmospheric visibility and turbidity," *Atmospheric Research*, vol. 96, no. 4, pp. 496–509, 2010.

[24] X. X. Li, T. T. zhou, H. J. Zhao et al., "The correlation of visibility and meteorological elements and the typical case over Dalian during 2010-2012," *Desert and Oasis Meteorology*, vol. 12, no. 4, pp. 65–73, 2018.

[25] J. H. Lv, Y. B. Peng, and G. Xie, "Relationship between visibility and relative humidity,PM10,PM2.5 in Jinan in 2013," *Meteorological and Environmental Sciences*, vol. 39, no. 4, pp. 93–97, 2016.

[26] Y. Li, Q. L. Chen, H. J. Zhao, L. Wang, and R. Tao, "Variations in PM10, PM2.5 and PM1.0 in an urban area of the Sichuan Basin and their relation to meteorological factors," *Atmosphere*, vol. 6, no. 1, pp. 150–163, 2015.

[27] Y. Q. Li, C. L. Lu, and X. H. Fan, "Fog forecast method in Jiaxing city," *Journal of Zhejiang Meteorology*, vol. 28, no. 1, pp. 14–17, 2007.

[28] W. F. Liang and Z. X. Hou, "Character and forecast of fog in qingdao area," *Journal of Shandong Meteorology*, vol. 2, pp. 16-17, 2001.

[29] H. C. Hu, H. D. Zhang, B. Zhu, and C. Xie, "Application analysis of neural network method in visibility forecast of coastal cities around Bohai Sea," *Journal of the Meteorological Sciences*, vol. 38, no. 6, pp. 798–805, 2018.

[30] J. Shu, Y. S. Duan, C. Y. Li et al., *Study on Forecast Model of Atmospheric Visibility in Shanghai*, Zhejiang Provincial Press, Zhejiang, China, 2004.

[31] X. W. Zhou, Q. G. Shi, J. M. Jia, and H. Q. Wu, "A method for classifying and forecasting low-visibility fog," *Journal of Tropical Meteorology*, vol. 30, no. 1, pp. 161–166, 2014.

[32] Y. P. Li, A. M. Liang, Z. F. Zhang et al., "Simulation and analysis of a winter advection fog in Beijing Area," *Journal of Yunnan University*, vol. 29, no. 2, pp. 167–172, 2007.

[33] A. C. W. Leung, W. A. Gough, and K. A. Butler, "Changes in fog, ice fog, and low visibility in the Hudson Bay Region: impacts on Aviation," *Atmosphere*, vol. 11, no. 2, pp. 186–219, 2020.

[34] T. M. Cover and P. E. Hart, "Nearest neighbor pattern classification," *IEEE Transactions on Information Theory*, vol. 13, no. 1, pp. 21–27, 1967.

[35] X. Q. Zeng, M. X. Shao, S. G. Wang, and H. Z. Liu, "Forecasting precipitation experiment with KNN based on crossing verification technology," *Journal of Applied Meteorological Science*, vol. 19, no. 4, pp. 471–478, 2008.

[36] M. X. Shao, H. Z. Liu, and Y. W. Dou, "Using nonparametric estimation technique to predict wind," *Journal Of Applied Meteorological Science*, vol. 17, pp. 125–129, 2006.

[37] X. P. Tu, S. R. Zhao, X. Q. Zeng, and H. Z. Liu, "Application of an updated KNN method to daily maximum wind forecast for coastal weather station from November to March," *Meteorological Monthly*, vol. 34, no. 6, pp. 67–73, 2008.

[38] Y. Y. Chen, H. Z. Liu, N. Chen et al., "Application of KNN to wind forecast based on clustering synoptic patterns," *Journal Of Applied Meteorological Science*, vol. 19, no. 5, pp. 564–572, 2008.

[39] B. Zhu, J. Yang, W. T. Lv et al., "Ground-based visible cloud image classification method based on KNN algorithm," *Journal Of Applied Meteorological Science*, vol. 23, no. 6, pp. 721–728, 2012.

[40] Y. J. Xiong, X. N. Liao, Z. M. Li et al., "Application of KNN data mining algorithm to haze grade forecasting in Beijing," *Meteorological Monthly*, vol. 41, no. 1, pp. 98–104, 2015.

[41] Y. J. Tang, D. Song, Y. X. Liu, and B. Liao, "Research on low-visibility weather classification forecasting procedure in motorway of Guizhou," *Journal of meteorological research and application*, vol. 36, no. 1, pp. 96–113, 2015.